Special Interest Group Meeting on Thermal Issues
ETH, Zurich, Switzerland, March 2022
www.euspen.eu

Influences of metalworking fluid on the thermal errors of a 4-axis thermal test piece

Sebastian Lang[1,3], Nico Zimmermann[1,2], Josef Mayr[1], Markus Bambach[3], Konrad Wegener[2]

[1]*inspire AG, Technoparkstrasse 1, 8005 Zurich, Switzerland*
[2]Institute of Machine Tools and Manufacturing (IWF), ETH Zurich, 8092 Zurich, Switzerland
[3]Advanced Manufacturing Laboratory, ETH Zürich, Technoparkstrasse 1, 8005 Zürich, Switzerland

lang@inspire.ethz.ch

Abstract
Thermally induced errors of machine tools can cause up to 75% of geometric errors on machined workpieces and are therefore a crucial precision defining factor on any produced part, which in turn has further effects on the performance of the produced part during its life cycle. In the machining process, metal working fluid fulfils many tasks and ensures beneficial cutting properties. It can have a significant impact on the thermal behaviour of machine tools. A thermal test piece is produced to identify the thermal errors of a rotary axis of a 5-axis machine tool under a thermal load consisting of rotating the C-axis for four hours and subsequently idling for four hours, once with metalworking fluid active during the C-axis movement and once without the use of any metalworking fluid. This test piece is produced in accordance to ISO/CD 10791-10:2020 in such a way that it allows for separating the thermal location error contributions of the main machine axes, and to infer on the effect of the thermal errors on the finished product. The metalworking fluid has a significant effect on the thermal behaviour of the analysed machine tool. In the analysed load, the thermal errors are reduced, when metalworking fluid is active due to reduced and homogenised temperatures. However, this cooling can also lead to a sign change of the thermal error. The asymmetric MWF drainage system design in the Y-direction leads to thermal errors that could not be observed if no metalworking fluid is used as otherwise the Y-direction behaves thermosymmetrically.

Thermal error, Metalworking fluid, Test piece, Machine tool, Metrology

1. Introduction

Thermal errors of machine tools (MT) is an area of research that has gathered more and more attention in recent years. This is due to the ever increasing accuracy at high productivities required by industrial applications. For example, the push to achieve sustainability requires increased energy efficiency of the final products and therefore repeatable accuracy during the production process, ideally at minimal energy consumption. Mayr et al. [1] describes the change of position and orientation and component errors of MTs experiencing thermal influences and concludes that up to 75% of geometric workpiece errors originate from thermal sources.

Control based compensation [2] can be used also with self-adapting inputs [3] to reduce the impact of thermal errors on the machine kinematics. Thermal error compensation models typically only consider the thermally induced deviations of the tool centre point. However, the impact on the workpiece itself needs to be quantified, necessitating the use of thermal test pieces (TTPs). These allow for an increased understanding of how thermal errors affect the accuracy of actually produced parts and not only the machine tool kinematics. Therefore, thermal test pieces are essential in the evaluation of the effectiveness of thermal error compensation strategies.

Mares et al. [4] used a TTP that was visually inspectable to validate their compensation model in Z-direction. Ibaraki et al. [5]. Various international standards relate to the evaluation of thermal errors of machine tools. ISO 230-12 [6] describes the process of producing test pieces on subtractive metal working machine tools. ISO 10791-10 [7] describes the evaluation of thermal distortions and contains two different thermal test piece geometries. The first is based on the pyramid shaped TTP proposed by Ibaraki et al. [8] while the second is based on the TTP developed by Wiessner and Blaser et al. [9, 10] and lays the foundation for the TTP analysed in this paper.

Metalworking fluid (MWF) is used in a wide variety of processes carried out on MTs. The comprehensive effects on the thermal behaviour has been recognised by research but remains an open research field [11–13], most likely because it is difficult to model the effect of the MWF on the transient temperature fields in the MT, the workpiece and the fixtures. Mayr et al. [14] showed an increase in the thermal errors as well as an overall thermal damping effect triggered by MWF. Blaser et al. [10] evaluated a TTP under the use of flood cooling, which was shown to have the largest thermal effect on the analysed MT previously investigated by Hernández-Becerro et al. [15].

This paper evaluates the TTP proposed in ISO 10791-10 [7] on a 5-axis MT with a focus on the rotary axis once with and once without the use of MWF, giving insights how the use of MWF impacts the accuracy of a produced part. The upper facets are used to compensate the geometric error of the lower facets. The measurement and evaluation of the angular TTP error along the B-axis is demonstrated using position weighted linear regression analysis.

2.1 Methodology

The test piece was produced according to ISO 10791-10 [7] on a 5-axis milling MT. In a first step the MT had been turned on and left idling until a steady state without load was reached. As the aim of the experiments is quantifying the effects if temperature changes during the applied thermal load and the effects of environmental temperature fluctuations. First a discrete R-Test as proposed by Blaser and Zimmermann et al. [2, 16] was executed to determine the position and orientation

errors of the MT defining the reference state. Subsequently the reference features of the TTP were produced. These reference features define the baseline of the thermal error of the MT as measured on the TTP. Every hour one set of features was produced, and the difference between the measurements in the reference state and the error measured was taken as a measure for the evolution of the thermal state of the MT. The TTP has to be measured after the experiment was carried through in order to be able to investigate the thermal errors as they would affect any produced part. If a sufficiently repeatable MT is available with a touch trigger probe this can be performed in the same clamping instead of a CMM as shown by Wiessner et al. [17]. In these experiments, the TTP measurement was always done on the subsequent day in the same clamped position, to ensure a reliable measurement without thermal or geometric effects influencing the TTP measurement. This requires a thermal steady state during the measurement, however as the thermal errors are calculated relative to the reference features this state does not have to be the initial reference state.

2.2. Thermal Test Piece

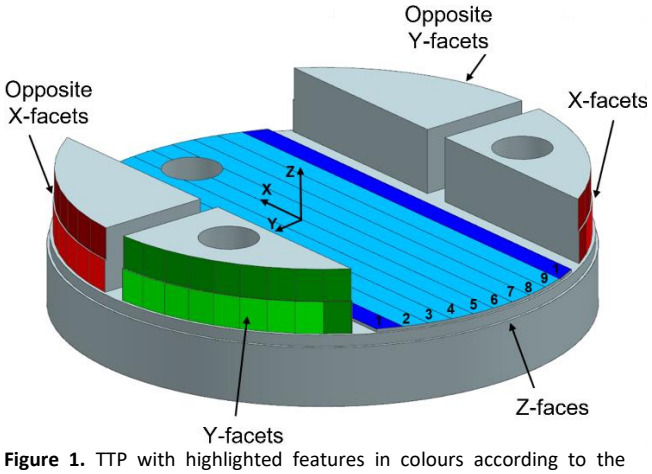

Figure 1. TTP with highlighted features in colours according to the respective thermal errors (red, green, blue ⇔ XYZ). The darker shades depict the reference features, the lighter colours depict the eight repetitions.

Figure 1 shows the TTP with the three features highlighted. The TTP is fixed on the MT table with three Ø10mm screws oriented in 120° angles along a concentric circle. The X- (red) and Y- (green) facets are highlighted as well and produced at a fixed Z- and X- or Y- position respectively by moving the Y-axis in case of the X-facet, and the X-axis in case of the Y-axis. In blue the Z-faces are highlighted which are produced at a fixed Z-position.

2.3. TTP Error definition and measurement procedure

Four distinct thermal errors can be measured and evaluated using the TTP. The X- and Y- thermal errors are measured using the deviation of the distance between the X- and Y-facet area mean points from the respective reference distance controlled by the respective upper facet for geometrical errors. For this each facet was measured using a touch trigger probe at 5 distinct points j $X_{j,n}$ positioned in the 4 corners of a smaller square of the facet with one in the centre of the facet. These data points were aggregated and the mean X or Y position was taken to calculate the distance from the opposing facet $d_{Xn}(t_i)$. The geometric errors at this position in the workspace are considered by referencing it to the respective upper facet yielding $\Delta d_{Xn}(t_i)$ .With $n \in [1,2]$ describing which X or Y-facet block is referenced, it holds that:

$$\Delta d_{Xn}(t_i) = \frac{\sum_{j=1}^{5}\left(X_{j,n,lower}(t_i)\right)}{5} - \frac{\sum_{j=1}^{5}\left(X_{j,n,upper}(t_i)\right)}{5} \quad (1)$$

$$E_X(t_i) = \frac{(\Delta d_{X2}(t_i) - \Delta d_{X2}(t_0)) - (\Delta d_{X1}(t_i) - \Delta d_{X1}(t_0))}{2} \quad (2)$$

$E_X(t_i)$ describes the measure thermal error on a workpiece in X direction with $t_i \in [0,8]$ referencing the respective timestep. Similarly for y:

$$\Delta d_{Yn}(t_i) = \frac{\sum_{j=1}^{5}\left(Y_{j,n,lower}(t_i)\right)}{5} - \frac{\sum_{j=1}^{5}\left(Y_{j,n,upper}(t_i)\right)}{5} \quad (3)$$

$$E_Y(t_i) = \frac{(\Delta d_{Y2}(t_i) - \Delta d_{Y2}(t_0)) - (\Delta d_{Y1}(t_i) - \Delta d_{Y1}(t_0))}{2} \quad (4)$$

All Z-faces are measured at five different X-coordinates at three different Y-coordinates while still remaining in one feature lane. For the Z-error these measurements are averaged and compared to the average of both reference faces:

$$d_Z(t_i) = \frac{\sum_{j=1}^{30}\left(Z_{meas,j}(t_i)\right)}{30} \quad (5)$$

$$E_Z(t_i) = d_Z(t_i) - \frac{d_{Z,1}(t_0) + d_{Z,2}(t_0)}{2} \quad (6)$$

The error E_B is also calculated using the Z-faces. A linear regression over all Z_{meas} along the X-axis is used to determine the angle β which allows to calculate the error E_B.

$$E_B(t_i) = \beta(t_i) - \frac{\beta_1(t_0) + \beta_2(t_0)}{2} \quad (7)$$

2.4. Experimental set up

The kinematic chain of the investigated machine tool, can be described according to ISO 10791-2 [18] as:
V [w–C2'–A'–X'–b –Y–Z–C1–t].

It is located in a not air-conditioned workshop. Initially, similarly to the procedure proposed by Wiessner et al. [9] the shape of the TTP is pre-machined out of a cylindrical block of aluminium leading to a TTP with a diameter of Ø160 mm.. After the reference R-test is carried through the reference TTP features are produced and the load case is started. In the first four hours the C-axis rotates continuously at maximum speed of 120 rpm representing the warm-up behaviour of the MT. In the experiment with active MWF during this time the MWF is supplied in the standard condition using the nozzles located in the spindle encasing focused on the cutting area. The used MWF is a water based emulsion. Subsequently the experiment is continued for another four hours without any axis movement simulating a cool down behaviour. Every hour the load case is interrupted, a set of features containing one Z-face and one pair of X- and Y-facets respectively is machined. This is followed by a discrete R-Test and the recording of various temperature sensors located inside and in the direct vicinity of the MT, before the load case is resumed for another hour. After eight hours nine feature sets are produced on the workpiece, the first measurement is defined to be the reference and all positions are measured relative to this position.

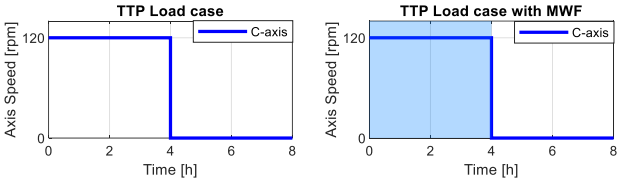

Figure 2. Load case of the TTP experiment with and without MWF.

3. Results and discussion

Figure 3 depicts the temperatures measured on the MT during the experiments. The experiment without MWF is performed in summer and with active MWF in winter to investigate different environmental conditions also. The C-axis temperature sensor is located inside the C-axis casing below the MT table close to the direct electrical drive. The sensor measuring the environment temperature is located in the air directly surrounding the MT on

a similar height as the working space temperature sensor around the top Z-position of the TTP. The working space temperature sensor is located inside the MT housing next to the table.

The largest variation is clearly visible in the C-axis temperature sensor, which is no surprise as the motor acts as the main heat source during the C-axis rotation. Before the start of the load cycle the temperature was below the ambient and even the working space temperature which is due to the active cooling of the motor. During the load cycle without MWF, the temperature increases by around 15° C, before slowly dropping back to a steady state slightly below the ambient temperature. In the load with MWF the C-axis temperature only increases by ~7° C and stays much more constant during the load cycle. Within one hour, it drops below ambient temperature after the C-axis movement is stopped. The working space temperature follows the ambient with a slightly reduced temperature as components in the MT are actively cooled and only little air is exchanged between the environment and working space. There is one notable exception of this difference which occurs right after the MWF is turned off and the working space temperature (1 hour after turning off) is reduced by around 1.5°C due to the evaporative cooling of the water based MWF which remains in droplets and film covering the MT inside and especially the chip conveyor.

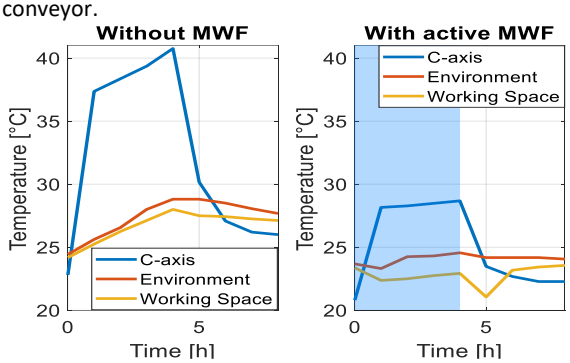

Figure 3. Temperature measurements sampled during the R-Test of both TTP experiments.

3.1 Thermal Error Results

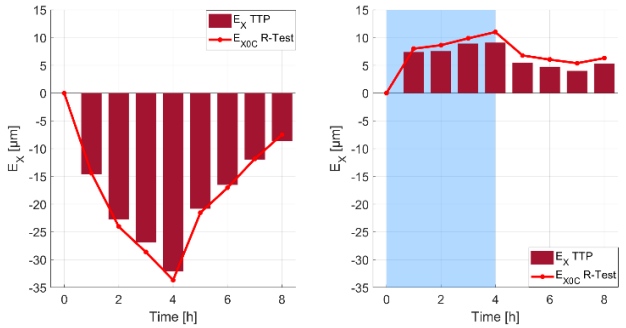

Figure 4. E_X thermal error of the TTP as well as the MT errors measured directly after the TTP production step.

Figure 4 illustrates the thermal error E_X as measured on the TTP and measured by the R-Test during the experiment directly. The difference between the R-Test results and TTP are only minimal and below 2 µm. This can be explained by the slight time shift between the R-Test measurement and the thermal influence arising during the feature production itself, however it is also close to the general measurement uncertainty of 1 µm of the employed MT. The use of MWF greatly reduces and homogenizes the E_X thermal error and even changes its orientation. The deviation between starting and finishing value is assumed to mostly originate from the changes in the environmental temperature.

Figure 5 depicts the thermal error E_Y. Again the agreement between the measured values from the TTP and the R-Test are very close together. In the dry case the thermal error E_Y is almost completely negligible, which is due to the symmetry plane the table has in Y-direction, which nullifies any thermal expansion at the centre point. However, in the case with MWF this is no longer the case as the MWF is only drained on one side and therefore only flows to this side where it accumulates in puddles and as a film in the drainage system. After the MWF is deactivated the thermal error drops rapidly before increasing slowly again. This shows the significance of thermal effects of the MWF, which cannot simply be generalised from only the dry case as the presumed symmetry plane only holds true under certain conditions, in this case the absence of MWF use.

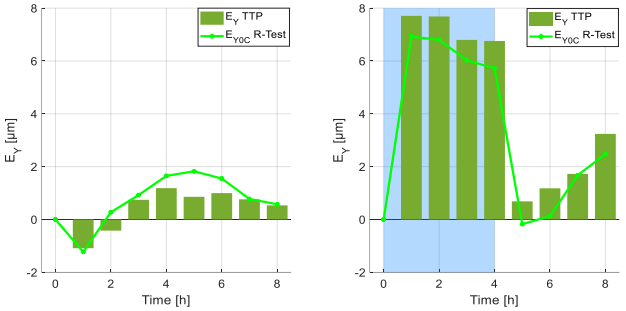

Figure 5. E_Y thermal error of the TTP as well as the MT errors measured directly after the TTP production step.

Figure 6 shows the thermal error E_Z. In this case the deviation between the R-Test and TTP is slightly larger but still clearly follows the same trend. However, as the TTP also encompasses the effects from both the tool and the workpiece the similarity is remarkable. The most significant part of the deviation can be observed during the cool-down phase, where the R-Test consistently measures a larger thermal error of almost constant 10 µm compared to the TTP. This may be due to the fact that the TTP feature set is produced before the R-Test is performed which acts as brief heat source on the spindle which is known to have a comparatively low thermal time constant and therefore reacts quickly. This can lead to an expansion of the spindle and as no steady state is reached, a deviation between the TTP and R-Test measurements are observed. Overall the error E_Z shows the largest magnitude as to be expected by a load case introducing heat into the table structure. The error profile correlates quite closely to the C-axis temperature depicted in Figure 2. As exemplified by the highest correlation coefficient for all thermal error temperature pairs of 0.9866 in the case without MWF and 0.9902 in the case with MWF indicating that the C-axis temperature would be a highly suitable predictor for the E_Z thermal error, at least in cases where there is a singular dominant heat source located in the C-axis. In the case without MWF a prolonged heating is observed, while in the case with MWF a steady state is already reached after the first feature production indicating a significantly lower thermal time constant.

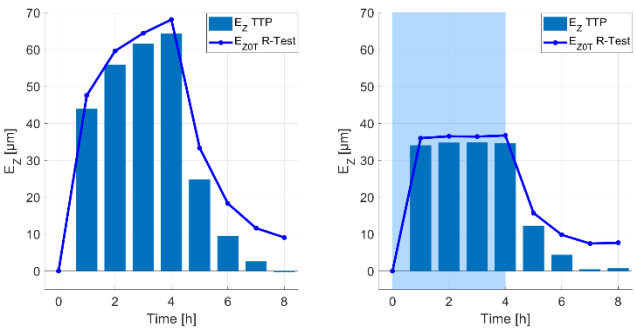

Figure 6. E_Z thermal error of the TTP as well as the MT errors measured directly after the TTP production step.

Figure 7 illustrates the thermal error E_B. Which is the angular thermal error rotated along the B-axis, therefore it is measured as an angle in µm/m with 30 measurement points over a total measurement length of 92 mm. It is clearly visible that this error has by far the biggest deviations between the R-Test and TTP, however the same general behaviour is still clearly observable. This deviation is likely due to various factors as the measurement uncertainty of the R-Test is only quantified with ~2.5 µm/m this cannot explain the variation. It can be seen that the fit uncertainty varies between the different features and becomes especially large at small thermal errors as the geometric errors become more significant (especially for the references). The easiest remedy would be adding more measurement points as well as increasing the overall measurement length which is rather short with only 92 mm. Increasing this measurement length would necessitate measuring closer to the edge of the TTP which was not possible yet in this design due to the location of the fixture hole as well as increasing the size of the TTP. However, the MT working space is still a restriction, especially with a precision sphere mounted eccentrically on the table little space is left if safety margins are required to prevent a crash during the experiment. Another notable fact is the quick variation of the thermal error due to the time delay between the machining of the respective feature and the R-Test as the facets are produced in between, which was also visible in the E_Z thermal error.

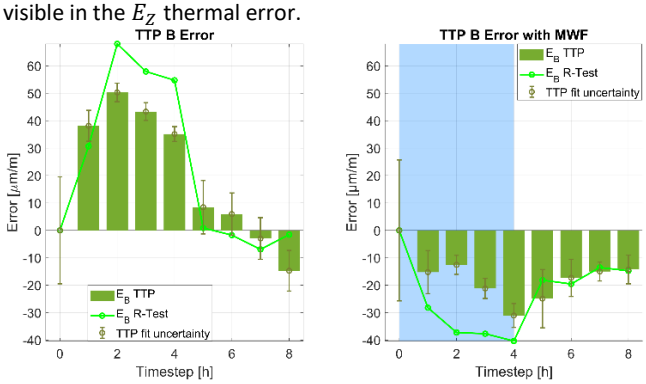

Figure 7. E_B thermal error of the TTP as well as the MT errors measured directly after the TTP production step.

4. Conclusion and Outlook

Using the two TTP, the influence of MWF on the thermal load case was shown. The angular error E_B was calculated using linear regression and compared to the R-Test. This comparison indicates acceptable agreement, despite the short measurement length. The use of water-based MWF reduced the temperature variation and the resulting thermal errors, in the case of the Z error by around 40%. It also leads to a quasi-steady state of the internal MT components quicker leading to reduced variation during the applied load. However, additional asymmetries may be introduced due to the use of MWF as well as strong transient effects at the start and end of the MWF use, due to the convection with the activated MWF or due to evaporative cooling in the use of water based MWF after the deactivation of the MWF use.

Additional research should focus on applying TTPs to validate the compensation methods, especially as the agreements of the on machine measurements to the errors seen on the workpiece was very high. This promises success in further research as a strong correlation between certain temperatures and the error was observable they may be a suitable predictor that requires no MT interruptions. Additional research on extending the TTP is however required as well. True compensated 5-axis machining requires the measurement and identification of additional errors as more axes are used and a separation of for example the effects originating from the table and the spindle becomes necessary if the production process happens in various table positions. The thermal positioning error of the linear axes requires additional study as well, especially for the use of larger working spaces.

References

[1] J. Mayr, J. Jedrzejewski E. Uhlmann, M. Donmez, W. Knapp, F. Härtig, K.Wendt, T. Moriwaki, P. Shore, R. Schmitt, C. Brecher, T. Würz, K. Wegener. “Thermal issues in machine tools,” *CIRP Annals*, vol. **61**, no. 2, pp. 771–791, Jan. 2012.

[2] P. Blaser, F. Pavliček, K. Mori, J. Mayr, S. Weikert, K. Wegener, “Adaptive learning control for thermal error compensation of 5-axis machine tools,” *Journal of Manufacturing Systems*, vol. **44**, pp. 302–309, 2017.

[3] N. Zimmermann, S. Lang, P. Blaser, J. Mayr, “Adaptive input selection for thermal error compensation models,” *CIRP Annals*, vol. **69**, no. 1, pp. 485–488, 2020.

[4] M. Mareš, O. Horejš, L. Havlík, “Thermal error compensation of a 5-axis machine tool using indigenous temperature sensors and CNC integrated Python code validated with a machined test piece,” *Precision Engineering*, vol. **66**, no. July, pp. 21–30, 2020.

[5] S. Ibaraki, Y. Ota_, “A machining test to calibrate rotary axis error motions of five-axis machine tools and its application to thermal deformation test,” *International Journal of Machine Tools and Manufacture*, vol. **86**, pp. 81–88, 2014.

[6] International Organization for Standardization (ISO) Geneva Switzerland, “ISO CD 230-12 Test code for machine tools — Part 12: Accuracy of finished test pieces,” 2020.

[7] International Organization for Standardization (ISO) Geneva Switzerland, “ISO CD 10791-10 Test conditions for machining centres — Part 10: Evaluation of thermal distortions,” 2020.

[8] S. Ibaraki, R. Okumura, “Machining tests to evaluate machine tool thermal displacement in z-direction: Proposal to ISO 10791-10,” *International Journal of Automation Technology*, vol. **14**, no. 3, pp. 380–385, 2020.

[9] M. Wiessner, P. Blaser, S. Böhl, J. Mayr, W. Knapp, K. Wegener, “Thermal test piece for 5-axis machine tools,” *Precision Engineering*, vol. **52**, no. February, pp. 407–417, 2018.

[10] P. Blaser, P. Hern, J. Mayr, M. Wiessner, “Cutting Fluid Influences - Evaluation With Thermal Test,” *Proceedings of the 32nd ASPE Annual Meeting 2017*, 2018.

[11] C. Brecher, F. Tzanetos, D. Zontar, “Investigation of the negative influence of cooling lubricants on the deformation of the machine tool structure,” *E3S*, vol. **95**, 2019.

[12] M. Braunig, J. Regel, J. Glanzel, M. Putz, “Effects of cooling lubricant on the thermal regime in the working space of machine tools,” *Procedia Manufacturing*, vol. **33**, pp. 327–334, 2019.

[13] T. Kizaki, S. Tsujimura, Y. Marukawa, S. Morimoto, H. Kobayashi, “Robust and accurate prediction of thermal error of machining centers under operations with cutting fluid supply,” *CIRP Annals*, vol. **70**, pp. 1–4, 2021.

[14] J. Mayr, M. Gebhardt, B. B. Massow, S. Weikert, K. Wegener, “Cutting fluid influence on thermal behavior of 5-axis machine tools,” *Procedia CIRP*, vol. **14**, pp. 395–400, 2014.

[15] P. Hernández-Becerro, P. Blaser, J. Mayr, S. Weikert, K. Wegener, “Measurement of the effect of the cutting fluid on the thermal response of a five-axis machine tool,” *Laser Metrology and Machine Performance XII*, 2017.

[16] N. Zimmermann, J. Mayr, K. Wegener, “Extended discrete R-Test as on-machine measurement cycle to separate the thermal errors in Z-direction,” 2020.

[17] M. Wiessner, P. Blaser, S. Böhl, J. Mayr, K. Wegener, “Test piece for thermal investigations of 5-axis machine tools by on-machine measurements,” in *Conference on Thermal Issues in Machine Tools: proceedings: CIRP sponsored conference, Dresden*, 2018, pp. 453–462.

[18] International Organization for Standardization (ISO) Geneva Switzerland, “ISO 10791-2:2001 Test conditions for machining centres — Part 2: Geometric tests for machines with vertical spindle or universal heads with vertical primary rotary axis (vertical Z-axis),” 2001.